IUST Iran University of Science and Technology

Iranian Journal of Electrical and Electronic Engineering

Journal Homepage: ijeee.iust.ac.ir

Research Paper

Empirical Analysis of Path Adjustment Factors for 10.982 GHz Slant Path and 14.8-15.3 GHz Terrestrial Radio Link

A.Y. Abdulrahman*(C.A.), O. S. Zakariyya*, A. S. Afolabi*, and A. T. Ajiboye**

Abstract: Rain attenuation prediction models are inevitably deployed to provide rough estimates of the actual measured attenuation due to severe scarcity in most of the tropical and equatorial climates. The results of rain attenuation measurements over a 14.8 GHz terrestrial microwave link and slant-path attenuation in vertically polarized signals propagating at 10.982 GHz in a tropical Malaysian climate were reported in this study. The experimental results including the path adjustment factors were compared with the predictions of some selected rain attenuation models. The relative errors in the path length adjustment factors (PLAFs) are in the range -0.3370 – 2.6272, while those of the slant path adjustment factors (SPAFs) are -0.9252 – +0.2923. Moreso, the charts of PLAFs and SPAFs at 0.01% of the time were also presented because they are the most commonly used availability by the telecommunications service providers. This study will allow the radio engineer to select the most suitable prediction models for the particular region under study, thereby ensuring adequate radio planning for improved service delivery especially in the tropical climates due to their peculiarity.

Keywords: Effective Rain Height, Extrapolation Function, Pathlength Adjustment Factor, Slant Path Adjustment Factor, Vertical Structure of Rainfall.

1 Introduction

RAIN-INDUCED attenuation above 10 GHz can be severe at heavy rain rates over both terrestrial and satellite links, thereby resulting in deep fading which can negatively impact on the quality of receive signal level, RSL [1, 2].

Iranian Journal of Electrical and Electronic Engineering, 2023.

Paper first received 09 Dec 2022, revised 26 May 2023, and accepted 26 May 2023.

*The authors are with Department of Electrical and Electronics Engineering, University of Ilorin, Ilorin, Nigeria, P. M. B. 1515, Ilorin, Kwara State, Nigeria.

E-mails: dareyyusuf@unilorin.edu.ng, zakariyya.os@unilorin.edu.ng and afolabisegun@unilorin.edu.ng.

**The author is with Department of Computer Engineering, University of Ilorin, Ilorin, Nigeria. P. M. B. 1515, Ilorin, Kwara State, Nigeria.

E-mail: ajiboye.at@unilorin.edu.ng.

Corresponding Author: A.Y. Abdulrahman.

https://doi.org/10.22068/IJEEE.19.3.2740.

Attenuation can be measured directly, or roughly estimated from prediction models. However, due to scarcity of direct measurement data in most of the tropical and equatorial climates, the prediction models are inevitably deployed to provide rough estimates of the actual measured attenuation.

In nearly all the rain attenuation prediction models, the major variable which is usually manipulated is the correction factor [3]. It is called *PLAF* for the terrestrial, or *SPAF*, for the satellite link. The specific rain attenuation is normally unaltered in the rain attenuation prediction models, so *PLAF* and *SPAF* are the major yardsticks for comparing rain attenuation prediction models.

The *PLAF* accounts for the inhomogeneities of rain on the entire propagation path for the terrestrial links. Also for the satellite links, the *SPAF* accounts for both the non-uniformity of rain rate in the horizontal direction and the effects of the non-uniform vertical structure of rainfall [4]. The latter is usually considered in the expression for the effective rain height.

A handful of rain attenuation prediction models for both terrestrial and satellite links exist in the literature; even though the ITU-R methods have the greatest global popularity. The expressions for *PLAF* and *SPAF* can be deduced from these models.

Different versions of the ITU-R prediction methods [5] have provided a methodological procedure for calculating the attenuation experienced by terrestrial links inserted in a rain-filled propagation path. In the most recent ITU-R prediction methods, the *PLAF* is expressed only in terms of rain rate, path length and the propagating frequency. The predictions of the ITU-R method are valid for path lengths up to 60 km for frequencies up to 40 GHz.

The new expression for *PLAF* yields significant improvement over the older expressions which were originally based on two assumptions [4]. One, the spatial structure of the rain was modelled by an equivalent rain cell, having a rectangular cross section of length. Two, the rectangular cross section of the equivalent rain cell can assume any position with respect to the path.

For satellite links inserted in a rain-filled propagation slant path, a constant rain height is assumed in the ITU-R prediction methods [6], which leads to inaccuracies. In reality, the rain height varies with rainfall rate, thereby taking care of the peculiarities of tropical and equatorial climates. However, it is quite difficult to measure the actual value of the rain height, so its formula is usually incorporated in most of the slant path attenuation prediction models.

Another issue is, the complex parameter "0.01%" recommended by the ITU-R models for determining attenuation over both terrestrial and satellite links is not a physical quantity. So, it is not obviously related to the dynamics of rain structure, as referred in [7]. Lastly, the attenuation $A_p(dB)$ exceeded for other probability levels, $(0.001\% < p < 1\%)$ is obtained by using an extrapolation function based on the value of attenuation $A_{0.01}(dB)$ exceeded at 0.01% of the time.

As referred in [4], the extrapolation procedures will normally result in a scenario where the same rain attenuation will be predicted for two regions with different rainfall rate regimes but similar values of$A_{0.01}$. Even though the most recent versions of the ITU-R methods have significantly improved the predictions of rain attenuation, there is still a room for further improvement, based on the aforementioned issues.

In practice, both the *PLAF* and *SPAF* are most conveniently determined by experimental approach, from the knowledge of attenuation along the rain-filled path length/slant path, propagating frequency and rain rate. Two sets of measurement results from a tropical Malaysian climate are reported in this study. First, the PLAFs derived from the measurement results of rain rate and attenuation over a 14.8 GHz terrestrial microwave link are compared to models' predictions. Secondly, the *SPAFs* derived from the measurement results of rain rate and slant path attenuation in vertically polarized signals propagating at 10.982 GHz are also compared to models' predictions.

2 Background

2.1 Path Length Adjustment Factor for the Terrestrial Link

Rain attenuation over a terrestrial microwave path can be obtained either by direct measurement, or predicted from the knowledge of the link path length and horizontal distribution of the rain along the path [8, 9]. The attenuation $A_p(dB)$ exceeded at p% of time is given by:

$$A_p = \gamma_R \, d_{eff} \tag{1}$$

where $\gamma_R = kR_p^{\alpha}(dB/km)$ is the specific rain attenuation for the rainfall rate $R_p(mm/h)$ exceeded at % p of time, while $d_{eff} = d.r$ (km) is the effective path length, defined as the product of the actual path length d (km) and *PLAF, r*. The values of parameters k and α can be obtained from the ITU-R method referred in [10], depending on the signal propagating frequency and wave polarization. The *PLAF* accounts for the inhomogeneities of rain on the entire propagation path. A brief review of some rain attenuation prediction models are presented, from which the respective formulas for the *PLAF* are derived.

2.1.1 ITU-R Prediction Method

The attenuation $A_{0.01}(dB)$exceeded at 0.01% is expressed as [5]:

$$A_{0.01} = k\,(R_{0.01})^{\alpha}\,d\,r_{0.01} \tag{2}$$

where $R_{0.01}$ and $r_{0.01}$ are the rain rate and *PLAF*, exceeded at 0.01%, respectively, while f (GHz) is the signal propagating frequency and d (km) is the path length.

$$r_{0.01} = \left[\frac{1}{0.477\left(d^{\,0.633}\right)R_{0.01}^{\,0.073.\alpha}\,.f^{\,0.123} - 10.579\left[1-\exp\left(-0.024.d\right)\right]}\right] \tag{3}$$

2.1.2 Lin Model

As referred in [11], the *PLAF* is expressed as:

$$r = \frac{1}{1 + d/d_0(R_p)} \tag{4}$$

$$d_0(R_p) = \frac{2623}{R_p - 6.2}km \tag{5}$$

where d_0 (km) is the diameter of rain cell. Note that r accounts for the partially correlated rain rate R_p variations along the propagation path length d. The value of *PLAF* is 0.5 when $d_0 = d(R_p)$. The model was formulated, based on measured distributions of 5-minute point rain rates and 11 GHz rain attenuation on 42.5 km path at palmetto, Georgia.

2.1.3 Revised Moupfouma Model

A terrestrial microwave link is characterized by its actual relay path length d that corresponds to the space between two ground stations, as referred in [12]. Hence, the equivalent propagation path length d_{eff}, is the product of the actual path length d and an adjustment factor, r, as defined in Eq. (6).

$$d_{eff}(R_{0.01}, d) = d\exp\left(\frac{-R_{0.01}}{1+\xi(d)R_{0.01}}\right) \tag{6}$$

The corresponding *PLAF* is given in Eqs. (7) and (8).

$$r = \exp\left(\frac{-R_{0.01}}{1+\xi(d)R_{0.01}}\right) \tag{7}$$

$$\xi(d) = \begin{cases} -100; & d \le 7km \\ \left(\frac{44.2}{d}\right)^{0.78}; & d > 7km \end{cases} \tag{8}$$

2.1.4 Revised Silva Mello Model

The method of using full rainfall rate distribution as input for predicting the rain attenuation cumulative distribution function (CDF) was employed in [4]. This is to improve the ITU-R limitations, as expressed in Eq. (9).

$$A_p = k\left(R_{eff}(R_p, d)\right)^{\alpha}\,.\,\frac{d}{1 + d/d_0(R_p)} \tag{9}$$

where d and R_p are the path length and rainfall rate exceeded at $\%p$, respectively.

The effective rain rate, $R_{eff} = 1.763R_p^{0.753+0.197/d}$ and the equivalent rain cell diameter $d_0(R_p) = 119R_p^{-0.244}$. The numerical coefficients were obtained by multiple non-linear regressions, using the measurement data in the ITU-R databanks. It is observed that the second term of Eq. (9) corresponds to the *PLAF*, where the equivalent diameter of rain cell, d_0 is numerically defined in Eq. (10).

$$r = \frac{1}{1 + d/119R_p^{-0.244}} \tag{10}$$

2.1.5 Dissanayake Model

Dissanayake et al. model [13, 14] was based on log normal distribution of rain rate and rain attenuation; and it is employed for terrestrial links. The model is approximately similar to the ITU-R model since the rain related input to the model is the rain intensity at 0.01 % of the time. The model is applicable within the frequency range 4-35 GHz. The horizontal *PLAF* at 0.01 % of the time, $r_{0.01}$ is given as:

$$r_{0.01} = \frac{1}{1 - 0.38\left[1 - e^{(-2d)}\right] + 0.78\sqrt{\frac{d\,\gamma_{0.01}}{f}}} \tag{11}$$

where d (km), $\gamma_{0.01}$ (dB/km) and f (GHz) are the path length, specific rain attenuation at 0.01% of the time and microwave link operating frequency, respectively.

Note that only the *PLAF* at 0.01% of the time, $r_{0.01}$ is provided in the ITU-R, DAH and Moupfouma models. To compute its values, r_p for other percentages of time, $\%p$, the ITU-R extrapolation formula in [5] was slightly modified, as given in Eq. (12) [15]:

$$r_p = \left[\frac{R_{0.01}}{R_p}\right]^{\alpha} \times r_{0.01} \times C_1\left(\frac{p}{0.01}\right)^{-(C_2 + C_3\log_{10}p)} \tag{12}$$

The formulas for estimating the coefficients, C_1, C_2 and C_3 are available in [5], as given in Eqs. (13a-13d):

$$C_1 = \left(0.07^{C_0}\right)\left[0.12^{(1-C_0)}\right] \tag{13a}$$

$$C_2 = 0.855C_0 + 0.546(1 - C_0) \quad (13b)$$

$$C_3 = 0.139C_0 + 0.043(1 - C_0) \quad (13c)$$

$$C_0 = \begin{cases} 0.12 + 0.4\left[\log_{10}(f/10)^{0.8}\right] & f \geq 10\,GHz \\ 0.12 & f < 10\,GHz \end{cases} \quad (13d)$$

2.2 Slant Path Adjustment Factor

2.2.1 Basic Formulas

The slant path attenuation $A_{p,s}$ (dB) exceeded at p% of time is given as [8, 9]:

$$A_{p,s} = \gamma_R L_{eff} \quad (14)$$

where the effective slant path L_{eff} (km) is defined as the product of slant path, L_s (km) and horizontal reduction factor, r_h; that is, $L_{eff} = L_s . r_h$. Now, expressing L_s in terms of effective rain height h_r (km), station mean altitude above the sea level h_s (km) and path elevation θ (degrees), as follows:

$$L_S = \frac{h_R - h_S}{\sin\theta} \quad (15)$$

Then, r_h is given in Eq. (16) as:

$$r_h = \frac{L_{eff} . \sin\theta}{h_R - h_S} \quad (16)$$

For a special case of 90° elevation path, when the receiver is pointed directly at the satellite, and since $h_R >> h$, Eq. (17) then reduces to:

$$r_h = \frac{L_{eff}}{h_R} \quad (17)$$

Note that the reduction factor ($r_h \leq 1$) accounts for the non-uniformity of the rain rate in the horizontal direction, while the effective rain height h_R accounts for the effects of the non-uniform vertical structure of rainfall. However, it is quite difficult to determine either r_h or h_R individually. The most convenient method is to determine the SPAF experimentally, which accounts for both the non-uniformity of rain rate in the horizontal direction and the effects of the non-uniform vertical structure of rainfall. The SPAF ψ_p exceeded at p% of the time is derived experimentally from Eqs. (14) -(16), as shown in Eq. (18).

$$\psi_p = \frac{A_{p,s}}{k R_p^{\alpha} L_s} \quad (18)$$

2.2.2 ITU-R model

The SPAF at 0.01% of the time, $\psi_{0.01} = r_{0.01} \times v_{0.01} =$ for the ITU-R methods, where $r_{0.01}$ and $v_{0.01}$ are the horizontal and vertical adjustment factors, respectively; and their formulas can be found in [6]. To compute the SPAFs for other percentages of time, p% the ITU-R extrapolation formula was slightly modified, as given in Equations (19a – 19c) [15]:

$$\psi_p = \left[\frac{R_{0.01}}{R_p}\right]^{\alpha} \times \psi_{0.01} \times \left(\frac{p}{0.01}\right)^{\lambda} \quad (19a)$$

$$\lambda = 0.655 + 0.033 \times \ln(p) - 0.045 \times \ln(A_{0.01}) - \beta(1-p)\sin\theta \quad (19b)$$

$$\beta = -0.005(|\varphi| - 36) \quad (19c)$$

Where φ is the latitude of the receiver ($< 36°$) and θ is the elevation angle ($\geq 25°$). The actual slant path is multiplied by ψ_p to give the effective slant path required in the computation of rain attenuation at time percentage p%, that is $L_{eff} = L_s . \psi_p$.

2.2.3 Svjatogor Model and Others

In [16], the effective rain height, h_R is expressed as:

$$h_R = \frac{2.7}{((\log_{10}(0.3R_p + 1.5)) + (0.0015R_p))} \quad (20)$$

$$Y = -0.0045 R_p^{0.68} \left(\frac{h_R}{\tan\theta}\right)^{0.6} \quad (21)$$

The horizontal adjustment factor, r_H is given as,

$$r_h = \exp(Y) \quad (22)$$

The mathematical descriptions of a few other prediction models are available in [4, 6, 17–24]. The values of SPAF are provided only at 0.01%, $\psi_{0.01}$ in some of the referred models. Therefore, their values, ψ_p for other percentages of time, p% may be computed by using Eqs. (19a) – (19c).

3 Measurement Setup

The long-term rain rate and rain attenuation measurements over the terrestrial and satellite links are presented in this section. The site for data collections was Islamic International University of Malaysia, IIUM, Kuala Lumpur, the capital city of Malaysia.

3.1 Rainfall Rate

The point rainfall rate with 1-minute integration time was measured using a tipping bucket arrangement of diameter 20-cm with 0.5 mm sensitivity. The rain gauge had its own programmable data logger which records the time of each tip to an accuracy of 0.1 s. The clock of the logger was regularly synchronized with that of the computer at every 10-s time interval to retrieve better data resolution. The gauge was calibrated in the laboratory by using a water measuring tube which can precisely measure 0.5 ml of water. Detailed descriptions are available in [3, 25].

3.2 Rain Attenuation over Terrestrial Microwave Link

The 1-s rain attenuation data were collected from a terrestrial microwave links of DiGi Telecommunications Sdn. Bhd., Malaysia [3, 25]. The microwave system consists of a microwave MINILINK operating at 14.8 GHz. The MINILINK was incorporated with data acquisition and processing system. Both transmit and receive antennas are horizontally polarized (i.e, the elevation angle is zero degrees, approximately) and were covered with radomes during the attenuation measurements. The path length between the transmit and receive antennas is 3.96 km, and they were so carefully positioned to ensure that the radiation pattern is such that the sidelobes are not pointing to the ground; that is the sidelobes receive insignificant level of noise (ground contamination). Note that the link path length was erroneously reported as “4.85 km” in [25].

The dynamic range of the maximum RSL is nearly 50 dB for excess (i.e. rain) attenuation; which is adequately suitable for the entire dynamic range of rain attenuation for this study. Wet antenna attenuation was also extracted from the actual measured attenuation so as not to contaminate the latter. More so, scintillations and other atmospheric absorptions along the propagation path were neglected in the study. The specifications of the MINI-LINKs, with 99.95 %, are shown in Table 1.

3.3 Rain Attenuation over the Slant Path

A measurement system was set up for monitoring ASTRO/MEASAT-3 beacon signal level [26]. The receiver site was located on the roof top of the Electrical and Computer Engineering building at IIUM in Kuala Lumpur. The receiver antenna is an off-set parabolic antenna dish with a diameter of 2.4 m; and it was pointed towards MEASAT-3, situated at 91.5° E (geostationary). The beacon signal is vertically polarized with a propagating frequency of 10.982 GHz. The Ku-band beacon signal is down-converted to an intermediate frequency (IF) signal (1.232GHz) using a low noise block (LNB) converter having a noise figure of 0.3dB. The down-converted signal (i.e., the output at LNB) was fed to a spectrum analyzer via RG-11 coaxial cable, at a sampling rate of 0.1 sample/s. The spectrum analyzer output was fed to computer via General purpose interface bus (GPIB) cable and then stored using a data logger developed by LabVIEW at same sampling rate (0.1 sample/s). The propagation characteristics of Kuala Lumpur are shown in Table 2, while the picture illustrating the communication link, the elevation angle and the length of the path in the rain is presented in Fig. 1.

Table 1 Specifications of the DIGI MINILINK.

Type of antenna	Front-fed parabolic	
Frequency band (GHz)	14.8 – 15.3	
Polarization	Horizontal	
Maximum transmit power (dBm)	+18.0	
10^{-6} BER (2X2 Mbps) Receive threshold (dBm)	-84.0	
Antenna beam width (degrees)	2.3	
Dynamic range (dB)	50	
Antenna for both	Size (m)	Gain(dBi)
Transmit and receive side	0.6	37.0

Table 2 Site propagation characteristics.

Measurement site	Kuala Lumpur, Malaysia 3.1390°N; 101.6869°E
Frequency (GHz)	10.982
Polarisation	Vertical
Antenna elevation (degs)	77.400
Altitude (m)	21.950
(mm/h) $R_{0.01}$	133.0000

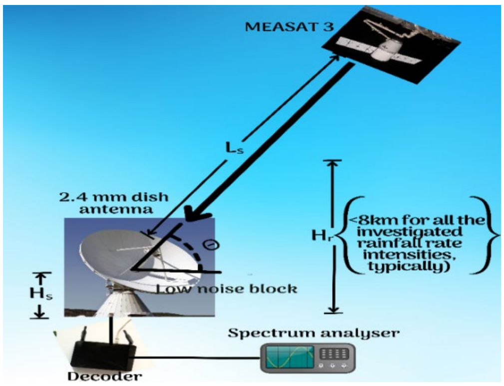

Fig. 1 A simple picture illustrating the communication link, the elevation angle and the length of the path.

The dynamic range of the maximum RSL is about 40 dB for excess (i.e. rain) attenuation, which adequately covers the entire dynamic range of rain attenuation for this study. The maximum value of measured rain attenuation is 35.9 dB at 0.001% of the time, which occurs at rain rate of 200 mm/h. The receive beacon signal is composed of rain attenuation and tropospheric scintillation. The scintillation effect was removed by filtering a time series of a received satellite signal using a LPF with a cut-off frequency of 25 mHz as shown in Equation (23) [26–27]. This is to allow precision in measurement of rain attenuation.

$$A(t)=\frac{1}{t_a}\sum_{t-t_a}^{t_a} A_r\,(t) \tag{23}$$

Where $A_r(t)$ is the unfiltered raw measured attenuation and the moving average t_a is 10s.

4 Results and Discussions

The measurement data for both terrestrial and satellite links were analyzed to produce two sets of results, as reported in this section. First, the *PLAFs* derived from the measurement results of rain rate and attenuation over a 14.8 GHz terrestrial microwave link are compared to models' predictions. Secondly, the *SPAFs* derived from the measurement results of rain rate and slant path attenuation in vertically polarized signals propagating at 10.982 GHz are also compared to models' predictions.

The measured rainfall rate cumulative distribution functions CDF is shown in Fig. 2, based on long-term rainfall rate data. The maximum attenuation measurements for both links were taken at 0.001% of the time, which occurs at rain rate of 200 mm/h.

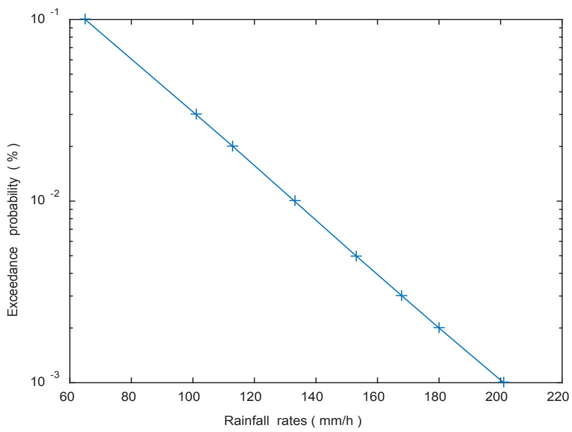

Fig. 2 Rain rates exceeded at p % of time.

4.1 Results for Terrestrial Microwave Link

The CDF of the measured rain attenuation over the 14.8 GHz terrestrial microwave link are compared to the model predictions, as shown in Fig. 3. The experimental values of *PLAF* were also compared to the predicted values, and their plots against rain rate are shown in Fig. 4. The charts of *PLAF* at 0.01% of the time are shown in Fig. 5.

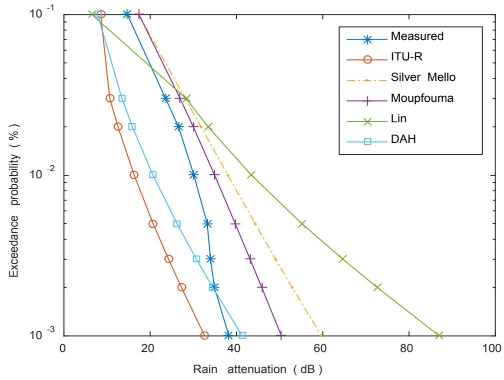

Fig. 3 Rain attenuation CDFs.

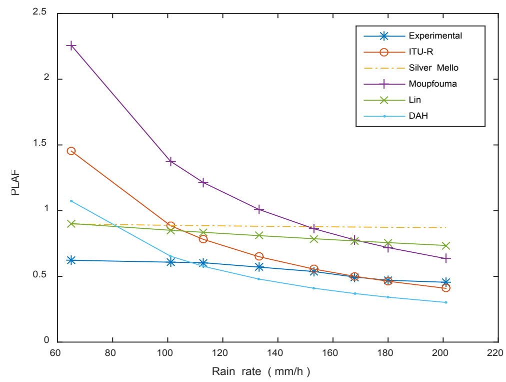

Fig. 4 Plots of PLAFs versus rain rates.

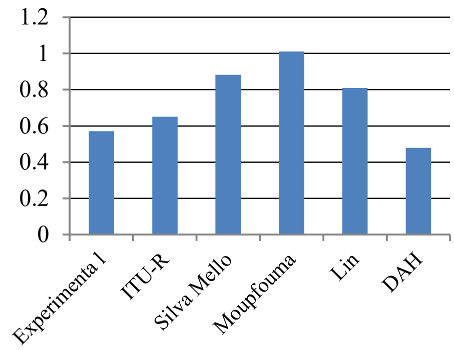

Fig. 5 Charts of PLAF at 0.01% of the time.

As shown in Fig. 3, the predictions of Silver Mello, Moupfouma and Lin models perfectly matched the measured attenuation at medium rain rates in the range 101-113 mm/h ($0.02\% < p < 0.03\%$). The three models produced low errors at low rain rates, below 101 mm/h ($R < 101mm/h$);

while they largely overestimated the measured attenuation at high rain rates greater or equal to 133 mm/h ($R > 133mm/h$). The measured attenuation was largely underestimated for nearly all percentages of time by both DAH and ITU-R models' predictions. The measured attenuation and DAH prediction almost coincided at 0.02% of the time, 34.94 and 34.53 dB, respectively. However, the measured attenuation at 0.01% of the time (38.24 dB) was slightly overestimated by the DAH model (41.33 dB).

As seen in Fig. 4, the PLAF decreases with increasing rain rate; and its experimental values and those predicted by Silver Mello and Lin models are generally less than unity for all percentages of time. The experimental values of PLAF are in the range $0.4552 < r \leq 0.6224$, while the predicted values are in the ranges $0.8706 < r \leq 0.8986$ and $0.7352 < r \leq 0.9019$ for the Silver Mello and Lin models, respectively.

On the other hand, the ITU-R, DAH and Moupfouma models exhibit some interesting behaviour, as the predicted values of PLAF are greater than unity ($r > 1$). This occurs at low rain rates, when $p \geq 0.1\%$ ($R \leq 65mm/h$) for the ITU-R and DAH models and when $p \geq 0.1\%$ ($R \leq 133\ mm/h$) for Moupfouma model. For example, values are in the range $0.4089 < r \leq 1.4534$, $0.3018 < r \leq 1.0726$ and $0.6352 < r \leq 2.2576$ for the ITU-R, DAH and Moupfouma models, respectively. These results are justifiable as it is sometimes necessary to make provisions for path reduction factors greater than unity ($d_{eff>d}$) as referred in [4] and [12]. As shown in Fig. 5, the values of *PLAF* at 0.01% of the time are less than 1.0, except for Moupfouma model which predicted 1.01.

4.2 Results for Satellite Link

The CDF of the measured slant path attenuation in vertically polarized signals propagating at 10.982 GHz was compared with the models' prediction, as shown in Fig. 6. Also, the experimental values of *SPAF* are compared to the predicted values, and their plots against rain rate are shown in Fig. 7. The charts of *SPAF* at 0.01% of the time are shown in Fig. 8.

As shown in Fig. 6, the measured attenuation was overestimated by the predictions of Ong and Nalinggam models for the entire percentages of time ($0.001\% < p < 1.0\%$). In contrast, the measured attenuation was underestimated by the predictions of Crane and SAM models for nearly all percentages of time. The predictions of the ITU-R, modified ITU-R, and Svyjatogor models are accurate at extremely low rain rates below 50 mm/h ($p \leq 0.5\%$). Ramanchrab and Moupfouma models predicted accurately at medium rain rates in the range 101–113 mm/h ($0.02\% < p < 0.03\%$) and 101–133 mm/h ($0.03\% < p < 0.01\%$), respectively. Bryant model predicted accurately only at high rain rates above 153 mm/h ($p \leq 0.005\%$).

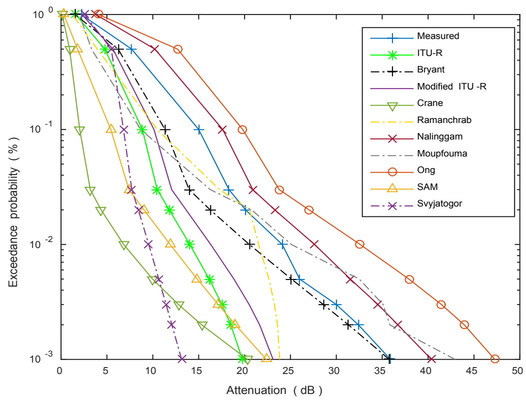

Fig. 6 Slant path attenuation CDFs.

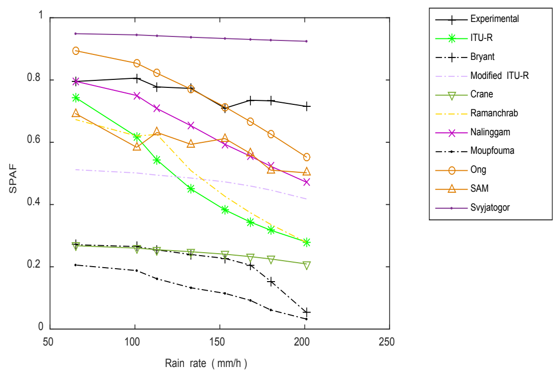

Fig. 7 Plots of SPAFs versus rain rates.

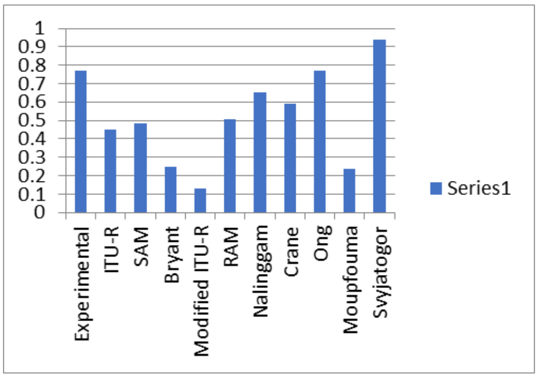

Fig. 8 Charts of SPAF at 0.01% of the time.

In Fig. 7, the *SPAF* decreases with increasing rain rate and its values are generally less than 1.0 ($r < 1.0$) for all percentages of time. The experimental values of *SPAF* were closely matched only by the predictions of Ong model, more specifically at very high rain rate in the range 133–180 mm/h ($0.002\% < p < 0.01\%$). The experimental values of *SPAF* were largely overestimated by the predictions of Svyjatogor model, while they were

Underestimated by others for all percentages of time. As seen in Fig. 8, the values of *SPAF* at 0.001% of the time are generally less than 1.0. Also, the modified ITU-R and Svyjatogor models predicted the highest and lowest values of the *SPAF*, 0.9374 and 0.1326, respectively.

4.3 Statistical Tests

The performance of each of the referred prediction models was statistically tested against the measured attenuation, using the percentage prediction error defined in Eq. (24) [15].

$$e_i = \frac{X_{pr}(p) - X_m(p)}{X_m(p)} \times 100 \qquad (24)$$

where $X_{pr}(p)$ is the predicted variable and $X_m(p)$ is the measured/experimental variable, and p denotes the percentage exceedance probability level at which the prediction error is calculated. The root-mean-square, *RMS,* error is given as

$$e_{rms} = \sqrt{\langle e_i^2 \rangle} \qquad (25)$$

where the averaging operator is denoted by $\langle\ \rangle$. The relative errors in the predicted *PLAFs* and *SPAFs* are plotted against their experimental counterparts, as shown in Figs. 9 and 10, respectively. More so, the corresponding charts of root-mean-square errors (%) are shown in Figs. 11 and 12, respectively.

As shown in Figs. 9 and 10, the relative errors are in the range -0.3370 to 2.6272 for the terrestrial link, while the range is -0.9252 to +0.2923 for the satellite link. Also, DAH and Moupfouma methods produced the lowest and highest R.M.S errors for the terrestrial link, while Ong model and SAM produced the lowest and highest for the satellite link, as shown in Figs. 10 and 11, respectively.

5 CONCLUSSIONS

The results of rain rate and attenuation measurements over both terrestrial and satellite links in a tropical climate were reported in this article. The accuracy and suitability of a few selected rain attenuation prediction models were tested against the measurement data; and the relative and rms errors of each of them have been reported. The experimental values of *PLAF* and S*PAF* were derived from the measurement data and compared with the predicted values. For the terrestrial link, DAH and Moupfouma methods respectively produced the lowest and highest R.M.S errors. The experimental values of the PLAF and those predicted by Silver Mello and Lin models are generally less than 1.0. In contrast, the values predicted by the ITU-R, DAH and Moupfouma are greater than 1.0.

For the satellite link, only the Ong model accurately predicted the *SPAF* among the ten considered models. More so, the Ong and SAM produced the lowest and highest R.M.S. errors, respectively. It is quite difficult to experimentally determine the horizontal reduction factor r_h and the effective rain height h_R individually. Therefore, it is more convenient to calculate the *SPAF*, which accounts for both the non-uniformity of rain rate in the horizontal direction and the effects of the non-uniform vertical structure of rainfall.

The charts of PLAF and SPAF were both highlighted at 0.01% of the time. This is because '0.01% is the most commonly used availability by the telecommunications service providers. Note that most of the inaccuracies observed in rain attenuation prediction models are inherently caused by the errors introduced in the modelling of the *PLAF* and *SPAF* of the terrestrial and satellite links, respectively. Therefore, the existing rain attenuation prediction models could be rigorously improved so as to minimize the associated prediction errors. Hence the study will ensure adequate radio planning for improved service delivery. Especially in the tropical climates where such data are very scarce.

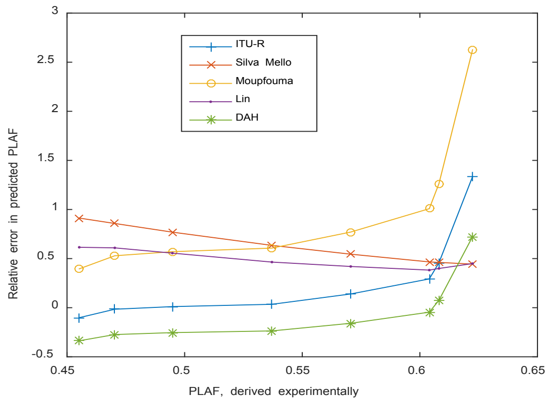

Fig. 9 Relative errors in the predicted PLAFs.

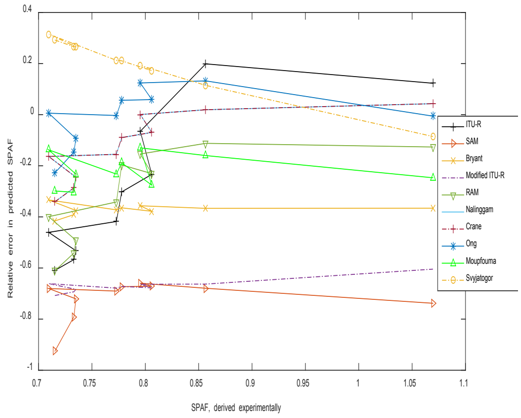

Fig. 10 Relative errors in the predicted SPAFs.

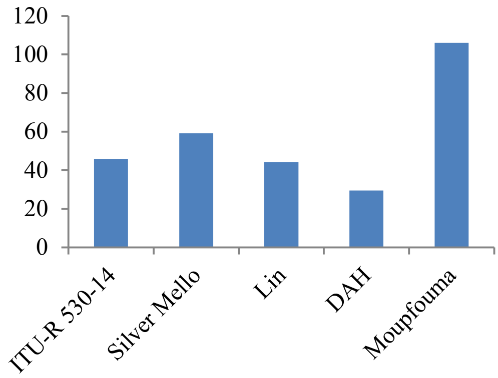

Fig. 11 % RMS errors in the predicted PLAFs.

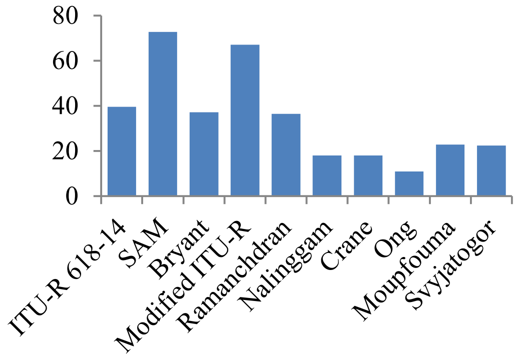

Fig. 12 % RMS errors in the predicted SPAFs.

Acknowledgement

This research is supported by the Antenna and Radio Propagation Group, (A&RPG), Department of Electrical and Electronics Engineering, University of Ilorin, Ilorin, Nigeria. Special thanks to Abdulhakeem Temitope Abdulrahman of CISTER Research Centre, ISEP Polythechinc Institute of Porto, Porto, Portugal (abdul@isep.ipp.pt) for helping in the analysis and preparation of the manuscript.

Intellectual Property

The authors confirm that they have given due consideration to the protection of intellectual property associated with this work and that there are no impediments to publication, including the timing to publication, with respect to intellectual property.

Funding

The research was funded by the Research Management Center (RMC), Universiti Teknologi Malaysia (UTM), Malaysia under the Post Doctoral Fellowship Scheme (Project Vote: 79382).

Credit Authorship Contribution Statement

A.Y. Abdulrahman: Data Curation, Conceptualization, Analysis, Software and Simulation **O. S. Zakariyya:** Original Draft Preparation, Revise & Editing. **A. S. Afolabi:** Software and Simulation. **A T. Ajiboye:** Revise & Editing, Verification.

Declaration of Competing Interest

The authors hereby confirm that the submitted manuscript is an original work and has not been published so far, is not under consideration for publication by any other journal and will not be submitted to any other journal until the decision will be made by this journal. All authors have approved the manuscript and agree with its submission to "Iranian Journal of Electrical and Electronic Engineering".

References

[1] P. M. Kalaivaanan, P. M., Sali, A., Raja S. A. R. A., Syamsuri Y., Mandeep J. S. and Ali, M. A, "On-The-Move Measurement Analysis for Ka-Band High Throughput Satellite and LiFi Communication Networks in Tropical Region", *IEEE Access*, Vol. 9, pp.71344 –71355, 2021.

[2] J. Polz, C. Chwal, M. Graf, and H. Kunstmann, "Rain Event Detection in Commercial Microwave Link Attenuation Data using Convolutional Neural Networks", *Atmospheric Measurement Techniques*, Vol. 13, pp. 3835-3853, 2020.

[3] A. Y. Abdulrahman, T. A. Rahman, S. K. A. Rahim, and M. R. Islam, "Empirically Derived Path Reduction Factor for Terrestrial Microwave Links Operating at

15GHz in Peninsula Malaysia", *Journal of Electromagnetic Waves and Applications*, Vol. 25, pp. 23- 37, 2011.

[4] L. da Silva Mello, and M. S. Pontes, "Unified Method for the Prediction of Rain Attenuation in Satellite and Terrestrial Links", *Journal of Microwaves, Optoelectronics and Electromagnetic Applications*, Vol. 11, No.1, pp. 1–14, 2012.

[5] Recommendation ITU-R P.530– 14, "Propagation Data and Prediction Methods Required for the Design of Terrestrial Line-of-Sight Systems", *ITU-R Radio Propagation Series*, 2012.

[6] Recommendation ITU-R P.618-14, "Propagation Data and Prediction Methods Required for the Design of Earth-Space Telecommunications Systems", ITU-R Radio Propag.Series, 2015.

[7] M. A. Ahmed, C. Michael, M. Marshed, H. A. Marwan and A. Yun, "Statistical Analysis of Rain at Millimeter Waves in Tropical Area", *IEEE Access*, Vol. 8, pp. 51044-51061, 2020.

[8] R. L. Freeman, "Eds., Radio System Design for Telecommunication", *3rd ed., United States: A Wiley Inter-science Publication*, Wiley, 2007.

[9] L. Luini, G. Roveda, M. Zaffaroni, M. Costa, and C. G. Riva, "The Impact of Rain on Short E-Band Radio Links for 5G Mobile Systems: Experimental Results and Prediction Models", *IEEE Transactions on Antennas and Propagation*, Vol. 68, No. 4, pp. 3124–3134, 2020.

[10] Recommendation ITU-R P.838–3, "Specific Attenuation Model for Rain for Use in Prediction Methods", *ITU-R Radio Propagation Series, Geneva, Switzerland*, 2005.

[11] S. H. Lin, "National Long Term Rain Statistics and Empirical Calculation of 11GHz Microwave Rain Attenuation", *The Bell System Technical Journal*, Vol. 56, No.9, pp.1581-1604, 1977.

[12]F. Moupfouma, "Electromagnetic Waves Attenuation due to Rain: A Prediction Model for Terrestrial or L.O.S SHF and EHF Radio Communication", *Journal of Infrared, Millimeter, and Terahertz Waves* Vol. 30, pp. 622–632, 2009.

[13] A. W. Dissanakaye and J. E. Allnutt, "Prediction of Rain Attenuation in Low Latitude Regions", *Proceeding of Undergraduate Research Summer Institute (URSI) Open Symposium. Ravenscar, United Kingdom (UK),* 1992.

[14] A. W. Dissanayake and N. J. McEwan, "Radar and Attenuating Properties of Rain and Bright Band," Proceedings. Part 2. (A80-15812 04-32) London, U.K., Institution of Electrical Engineers, (IEE), pp. 125–129, 1978.

[15] F. Minematsu, Y. Suzuki, M. Kamei and K. Shogen, "Comparison of Measured Rain Attenuation in the 12-GHz Band with Predictions by ITU-R Methods, *IEICE Transactions on Communications*, E88-B, No. 6, pp. 2419–2426, 2005.

[16] Cost Action 255 Final Report, "Radiowave Propagation Modeling for SatCom Services at Ku-band and above, ESA Publications Division, Nooedwijk, The Netherlands, 2002.

[17] G. H. Bryant, I. Adimula, C. Riva and G. Brussaard, "Rain Attenuation Statistics from Rain Cell Diameters and Heights", *International Journal of Satellite Communications*, Vol. 19, pp. 263–283, 2001.

[18] R. K. Crane, "Rain Attenuation Models: Attenuation by Clouds and Rain", *In Propagation Handbook for Wireless Communication System, CRC Press*, USA, pp. 225-280, 2003.

[19] J. X. Yeo, Y. H. Lee, and J. T. Ong, "Rain Attenuation Prediction Model for Satellite Communications in Tropical Regions", *IEEE Transactions on Antennas and Propagation*, Vol. 62, No. 1, pp. 5775–5781, 2014.

[20] F. Moupfouma, "Rain-induced Attenuation Prediction Model for Terrestrial and Satellite-Earth Microwave Links", *Annales des Télécommunications*, Vol. 42, pp. 539-550, 1987.

[21] R. Nalinggam, W. Ismail and J. S. Mandeep, "Comparison of Rain Attenuation Prediction Models with Ground Measurement Data for Penang", *IET Microwaves, Antennas and Propagation*, Vol. 5, No. 13, pp. 1546–1551, 2011.

[22] M. S. Pontes, L. A. R. Da Silva Mello, R. L. S. Souza and E. C. B. Miranda, "Review of Rain Attenuation Studies in Tropical and Equatorial Regions in Brazil", *In Proceeding of the 5th International Conference on Information, Communications and Signal Processing, (ICICSP '05). IEEE Explore*, Bangkok, Thailand, pp. 1– 4, 2005.

[23] V. Ramachandran, "Modified Rain Attenuation Model for Tropical Regions for Ku-Band Signals", *International Journal of Satellite Communications and Networking*, Vol. 25, pp. 53–67, 2007.

[24] W. L. Stutzman, and , K. M. Yon, "A Simple Rain Attenuation Model for Earth-

Space Radio Links Operating at 10-35 GHz", *Radio Sciences*, Vol. 21, No. 1, pp. 65–72, 1986.

[25] A. Y. Abdulrahman and A. T. Ajiboye, "Rain Fade Analysis and Link Budget Planning for 14.8 – 15.3 GHz Terrestrial Microwave Links Operating in Peninsula Malaysia", *Journal of Telecommunications and Radio Engineering*, Vol. 81, No. 8, pp. 43–59, 2022.

[26] A. Y. Abdulrahman, T. A. Rahman, M. R. Islam, B. J. Olufeagba and J. Chebil, "Comparison of Measured Rain Attenuation in the 10.982 GHz Band with Predictions and Sensitivity Analysis", *International Journal of Satellite Communications and Networking*, Vol. 33, No. 3; pp. 185–195, 2015.

[27] A. Y. Abdulrahman, "Comparison of measured slant path attenuation at 10.982 GHz with large-scale prediction models in a tropical climate". *Journal of Telecommunications & Radio Engineering*. 2023.

A. Y. Abdulrahman is a Reader in the Department of Electrical and Electronics Engineering, University of Ilorin, Nigeria. He obtained B. Eng and M. Eng degrees in Electrical Engineering in 1999 and 2005 respectively at University of Ilorin, Ilorin, Nigeria. He also had a PhD degree in Electrical Engineering from Universiti Teknologi Malaysia, (UTM), Malaysia in 2012. His areas of research interests include radiowave propagation, antenna measurements and designs.

O. S. Zakariyya is a is a Lecturer in Electrical and Electronics Engineering Department, University of Ilorin. He received his B.eng. degree in Electrical Engineering from Ahmadu Bello University Zaria, Nigeria in 2011, M.Sc. degree in Electrical and Electronics Engineering from Eastern Mediterranean University Cyprus and PhD degree in Telecommunications Engineering from Ahmadu Bello University Zaria, Nigeria in 2023. His research interests include but not limited to, Radio propagation, Antenna design, Wireless Communication Networks and Applications.

A. S. Afolabi received his Bachelor's and Master's Degrees in Electrical Engineering from the University of Ilorin, Nigeria in 2004 and 2009, and his Ph.D. Degree from Kobe University, Japan in 2012. He was the recipient of the prestigious Japanese Government MEXT Scholarship Award from 2009 to 2012. He is currently with the University of Ilorin. He has published numerous journal and conference papers and is fully registered with the Council for the Regulation of Engineering in Nigeria (COREN). His research interests include satellite communications, wireless sensor networks, and D2D communications.

A. T. Ajiboye Obtained a Bachelor of Science degree in Electrical Engineering from the University of Ibadan, Ibadan, Nigeria in 1989. He obtained a Master of Engineering degree and a Doctoral degree in Electrical Engineering from University of Ilorin, Ilorin, Nigeria in 2005 and 2012 respectively. He is a Reader in the Department of Computer Engineering, University of Ilorin, Ilorin, Nigeria and his research interests have been in Instrumentation and Control Systems design, simulation, and development. He can be contacted at email: ajiboye.at@unilorin.edu.ng.